



ChemComm

Chiroptical Anisotropy of Crystals and Molecules

Journal:	<i>ChemComm</i>
Manuscript ID	CC-FEA-02-2021-000991.R3
Article Type:	Feature Article

SCHOLARONE™
Manuscripts

COMMUNICATION

Received 00th XXXX 2021,
Accepted 00th XXXX 2021

Chiroptical Anisotropy of Crystals and Molecules

DOI: 10.1039/x0xx00000x

Alexander T. Martin,^{a,b} Shane M. Nichols,^{a,c} Veronica L. Murphy,^{a,d} Bart Kahr^{a*}

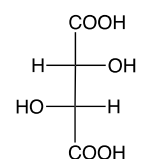
Abstract

Optical activity, a foundational part of chemistry, is not restricted to chiral molecules although generations have been instructed otherwise. A more inclusive view of optical activity is valuable because it clarifies structure-property relationships however, this view only comes into focus in measurements of oriented molecules, commonly found in crystals. Unfortunately, measurements optical rotatory dispersion or circular dichroism in anisotropic single crystals have challenged scientists for more than two centuries. New polarimetric methods for the unpacking the optical activity of crystals in general directions are still needed. Such methods are reviewed as well as some of the ‘nourishment’ they provide, thereby inviting to new researchers. Methods for fitting intensity measurements in terms of the constitutive tensor that manifests as the differential refraction and absorption of circularly polarized light, are described, and examples are illustrated. Single oriented molecules, as opposed to single oriented crystals, can be treated computationally. Structure-property correlations for such achiral molecules with comparatively simple electronic structures are considered as a heuristic foundation for the response of crystals that may be subject to measurement.

Anisotropy

Interrogations of molecular configuration by polarized light, a “most subtle and delicate investigator of molecular condition,”¹ remain essential to organic chemistry pedagogy,² yet no contemporary instructor can explain in words, for example, why the specific rotation of (2*R*,3*R*)-tartaric acid is +11 deg M⁻¹dm⁻¹ (at 589 nm and 295K).^{3,4} Since the discovery in 1815 that solutions of some compounds are optically active (OA – we use this acronym for *optically active* and *optical activity*, confident that the right meaning will be derived from the context),⁵ we have been unable to interpret

this response simply, thus perennially teaching students how to assign apparently random numbers – molar and specific rotations – to compounds. That said, legions of investigators have wrestled, often brilliantly, with chiroptical structure property relations of solutions. Progress of successive generations can be found in the monographs of Lowry,⁶ Mason,⁷ and Polavarapu,⁸ for example. For some compound types, incisive judgments about structure have been made.^{9,10} However, for many other compounds, like tartaric acid, the response of a molecule to linearly polarized light still cannot be reckoned in the classroom.



L-tartaric acid

Obstacles originate in both experiment and theory. 1. Optical rotation (OR) measured in solution is a pseudoscalar (signed) quantity, the average value of a second rank tensor. The fundamental response lies beneath the average which obscures the sufficient condition for OR.¹¹ 2. Electronic structures upon which light-matter interactions depend are complicated even for chiral molecules of only modest complexity. Computers can reckon with this complexity, but they do not narrate their answers. Unpacking averages and simplifying electronic structure are parallel paths to intuition. Given the important place of OA to the development of structural chemistry, we aim to deliver some intuition.

Challenges of Measurement

The rotation of the azimuth of linearly polarised light, OR in deg·mm⁻¹, and the related phenomenon of CD (typically in units of differential absorption or ellipticity), are bisignate quantities that depend on the interrogating wave vector with respect to the coordinate system of the molecule. In a solution, only average values are obtained. Unfortunately, the average value of an ensemble of ± numbers is not always instructive. Figure 1 shows schematically the typical measurement of a solution average over all orientations a small chiral molecule.

^a Department of Chemistry and Molecular Design Institute, New York University, New York City, NY, 10003, USA. Email: bart.kahr@nyu.edu

^b Americans for Financial Reform, 1615 L Street NW, Suite 450, Washington, D.C. 20036, USA

^c Johns Hopkins Applied Physics Laboratory, 1100 Johns Hopkins Road, Laurel Maryland 20723

^d Bethlehem Catholic High School, 2133 Madison Avenue, Bethlehem PA 18017

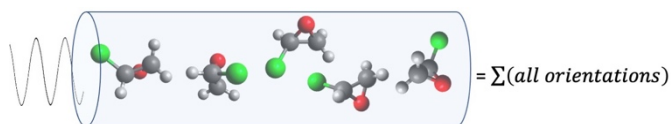


Figure 1. Measurement of OR over a random distribution of orientations of a chiral molecule gives the average value of individual contributions, some positive, some negative, some absolutely large, and others near zero.

To understand the relationship of structure and activity, it is necessary to characterize anisotropy by lining up molecules with respect to one another and arresting their reorientation. In this way, the wave vector of light can be specified and varied systematically with respect to molecules. There are many ways to partially orient molecules,^{12, 13, 14, 15, 16} however the surest way of aligning small molecules in the laboratory is to grow crystals. Thus, we arrive at the problem of OR and CD (together referred to as natural optical activity, or gyrotropy in the crystal physics literature) in single crystals. In fact, optical rotatory dispersion (ORD) was first observed for linearly polarised light along the high-symmetry *c*-axis of α -quartz more than two centuries ago, even before it was observed for molecules in solution.^{17, 18, 19, 20} However, measurement along a low-symmetry direction was stopped cold.

OR ($= \pi(n_L - n_R)d/\lambda$) arises in the circular birefringence (CB, $n_L - n_R$) and is manifest as a phase shift in radians where d is the thickness, λ is the wavelength, and n_L and n_R are respectively the refractive indices of left and right circularly polarized (CP) light. LB is the differential refraction of orthogonal *linear* polarisation states ($n_{\parallel} - n_{\perp}$) and can likewise be expressed as a phase shift. However, LB can be $\sim 10^3$ times larger than CB. The small effect may be obscured by the larger one. The underlying reason for the general difference in magnitude between LB and CB is simple. In calcite (CaCO_3),²¹ for example, a crystal that famously displays its LB (*ca.* 0.17) as Iceland spar, linear polarisation states can be fully aligned or anti-aligned with the highly polarisable C=O bonds in the parallel carbonate anions. This is manifest as big differences in refractivity experienced by the electric field vector polarised in or perpendicular to the the π bonds. However, in OA *guanidinium* carbonate²², CP light with helical arrangements of the electric field vectors, sample all directions normal to the direction of propagation. A difference in refractivity arises from the *spatial dispersion*²³ or variance of a dissymmetric crystal structure with lattice constants of several nanometers over the much larger electric field helix with a pitch of *ca.* 500 nm for visible light. In order words, a tiny tartaric acid molecule can barely detect the differences in helical light fields with pitches *ca.* $500 \times$ larger than the molecules themselves.

Along a high-symmetry direction, the optic axis in a uniaxial (trigonal, tetragonal, or hexagonal) crystal such as α -quartz, the anisotropy and associated LB disappears. In this circumstance, the differential interaction between quartz helices and CP light is slight. When the linearly anisotropies are obviated, the perturbations to CP states are more pronounced. However, it took 123 years for researchers to measure the OA of quartz along a low symmetry direction with non-

zero LB.²⁴ The determination of the quartz OR *anisotropy* and remains challenging today.^{25, 26}

Quartz OR has an orientational dependence as a function of the angle φ between the wave vector and the wave normal to the high symmetry axis. It is given in terms of two constants of anisotropy or tensor elements for light along the high symmetry (ρ_{33}) axis and for light perpendicular to it (ρ_{11}) such that the magnitude of OR as in Eq. 1:

$$OR(\varphi) = \frac{\pi d}{\lambda} (\rho_{33} \cos^2 \varphi + \rho_{11} \sin^2 \varphi), \quad (1)$$

It so happens that dextrorotatory quartz (positive OR along the easy direction) is *levorotatory* along the 'hidden' direction normal to the high symmetry *c*-axis; ρ_{11} and ρ_{33} are of opposite sign. Shubnikov made angular functions vivid by plotting the directional dependence of OR as a parametric surface in which the distance from the origin to the surface is proportional to the magnitude of OR in that direction, and the color or shading distinguishes the sign (Figure 2B).²⁷

ρ is a symmetric ($\rho_{ij} = \rho_{ji}$) second rank pseudo-tensor with six independent parameters that can be measured in a general direction of a dissymmetric crystal. It can then be diagonalized (Eq. 2). The average value, ρ_{ave} , corresponding to the solution rotation, is 1/3 of the trace of ρ_{symm} or ρ_{diag} (Eq. 3). Dissolution does this averaging for you, delivering a pseudo-scalar.

$$\rho = \begin{bmatrix} \rho_{11} & \rho_{12} & \rho_{13} \\ \rho_{12} & \rho_{22} & \rho_{23} \\ \rho_{13} & \rho_{23} & \rho_{33} \end{bmatrix}, \quad \rho_{diag} = \begin{bmatrix} \rho_{11} & 0 & 0 \\ 0 & \rho_{22} & 0 \\ 0 & 0 & \rho_{33} \end{bmatrix} \quad (2)$$

$$\rho_{ave} = \frac{\text{Tr}(\rho_{symm})}{3} = \frac{\text{Tr}(\rho_{diag})}{3} \quad (3)$$

There are two points of view in considering anisotropy, that of the wave vector, $k = 2\pi/\lambda$, and that of the mutually perpendicular field components. We have used both representations in the published work cited herein. Most studies of OA crystals use the wave vector convention. This builds the ρ_{ij} pseudo-tensor that can be scaled to units of OR in deg mm^{-1} . To treat light matter interactions in a consistent manner with other effects such as the dielectric permittivity ϵ_{ij} , we introduce the magneto-electric tensor α_{ij} , which becomes ρ_{ij} upon a symmetry-preserving matrix transformation.²⁸ For light traveling down the *c*-axis of quartz, the electric vector of the transverse light wave 'feels' the directions perpendicular to the optic axis, the high symmetry direction, therefore $\rho_{33} \propto 2\alpha_{11}$ ($\alpha_{11} = \alpha_{22}$ in quartz). Shown in Figure 2A are two OA crystal structures of ethylene diammonium sulfate (EDS) and its isostructural selenate (EDSe), and in Figure 2B and 2C are the representation surfaces for α and ρ , respectively.

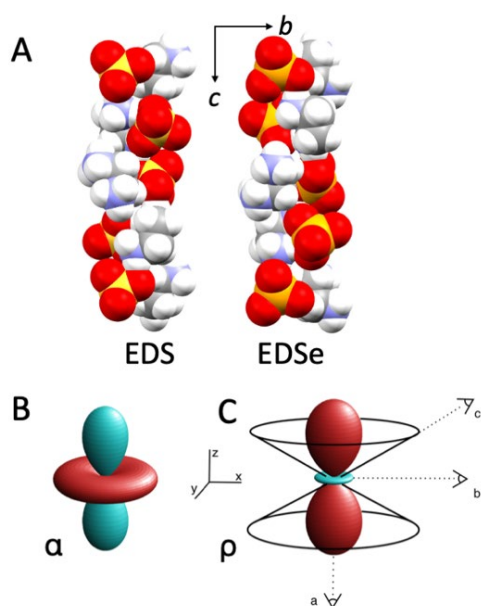


Figure 2. (A) Helical crystal structures of ethylenediammonium sulfate (EDS: $P4_12_12$, $a = b = 5.979(3)$ Å, $c = 17.991(9)$ Å) and ethylenediammonium selenate (EDSe: $P4_32_12$, $a = b = 6.1155(4)$ Å, $c = 18.132(1)$ Å) in enantiomorphous space groups. (B) Comparison of the normalized representation surfaces of the magnetoelectric tensor α (left) and of the ρ tensor (right). The cones represent the places where CB disappears. The dashed lines indicate viewing direction of the positive maximum (a), the negative minimum (b), and the null (c). Republished from ref. 153 with permission of International Union for Crystallography.

Theory

For many years, the interpretation of OA in crystals was grounded in classical polarisability theory^{29,30,31} because the quantum formula³² was difficult to apply. Classically, light waves induce dipoles on atoms of known positions and polarisabilities. The oscillations are then propagated in the material through dipole-induced dipole interactions. In suitably dissymmetric media, this leads to scattered radiation with a component of the electric field normal to the driving field, resulting in a change in the polarisation azimuth.³³ Some salts and minerals are reasonably approximated as sums of atomic polarisabilities,³⁴ but classical methods work less well for conjugated and aromatic molecules.³⁵

In the first decade of this century, quantum chemical calculations of OR were widely implemented for the *a priori* prediction of the interactions of CP light and matter.^{36, 37, 38, 39, 40, 41} These so-called linear response methods relied on the simulation of field-induced changes in expectation values for electric and magnetic multipole moments. The frequency-dependent linear response could be applied to wave function-based or density functional-based theories.⁴² They are widely incorporated in leading electronic structure computing programs, and predicting specific rotations of chiral compounds can be considered routine.^{43, 44} However, first principles studies invariably compute ρ_{symm} for an arbitrary molecular coordinate system (in asymmetric molecules) and are further reduced and reported commonly as ρ_{ave} , because we only have average values – molar or specific rotations – with which to make comparisons. Most of the information that is computed usually

is not reported. Exceptions include the trenchant work of Autschbach and coworkers^{45,46} which has emphasized the enabling role of anisotropy in interpretation. On the experimental side, Kuball and coworkers devoted a great deal of creative work to the analysis of CD anisotropy of analytes partially organized in mesophase carriers.^{14,47,48,49,50}

Quantum theoretically, OR measured at long wavelength is a sum of rotational strengths (R_{ij}^{0n})⁵¹ for all electronic excitations of frequency ω_{0n} for states $0 \rightarrow n$. This means that to compute ρ_{ij} one needs to know, in principle, all R_{ij}^{0n} that are embodied in Eq. 4,

$$OR \propto \rho_{ij} \propto \sum_{0 \neq n} \frac{R_{ij}^{0n}}{\omega_{0n}^2 - \omega^2}, \quad (4)$$

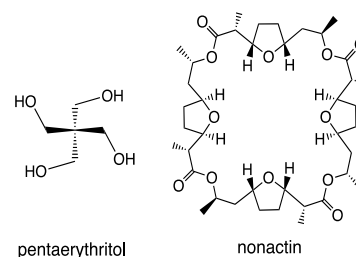
where ω is the frequency of the incident light. Two terms go into each R_{ij}^{0n} that the depend on coupling between transition electric dipoles μ_i and (1) transition magnetic dipoles (Eq. 5) and (2) transition electric quadrupoles (Q_{jk}) (Eq. 6) :

$$R_{ij}^{0n}(\mu, m) = \text{Im}\{\langle n | \mu_i | 0 \rangle \langle 0 | m_j | n \rangle\} \quad (5)$$

$$R_{ijk}^{0n}(\mu, Q) = \text{Re}\{\langle n | \mu_i | 0 \rangle \langle 0 | Q_{jk} | n \rangle\}. \quad (6)$$

Eq. 6 is averaged to zero over all orientations for solutions,⁵² however it contributes to crystals and oriented molecules. For some structures (below), it is small and can be ignored.⁵³

Even with a knowledge of the orientational dependence of OA of a single crystal, the interpretation on the basis of structure is not easy. This is because electronic structure is complicated, even for comparatively simple chemical systems. Knowledge of hundreds of excited state wave functions may be needed to account for OR of even the simplest chiral organic compounds, oxiranes as in Figure 1.^{54,55,56}



Alternatively, one can measure rotational strength or CD anisotropy, R_{ij}^{0n} ,^{57,58} but likewise it has experimental challenges, burdened as crystals are with linear dichroism (LD) (See List 1 for definitions). CD has been a viable method of analysis in isotropic solutions and for some crystals along optic axes only where LD=0 by symmetry.⁷

Pioneers

Following the 1934 analysis of quartz chiroptical anisotropy,²⁴ Federov^{59,60} and his students, in particular Konstantinova,^{61,62,63} contributed mightily to the measurement and formulation of OR (gyrotropy) of inorganic solids and with spectroscopic light sources for measurements of the oscillations of the transmitted azimuth of

elliptically polarized light as a function of wavelength.^{64,65,66,67,68} Interpretation was aided by classical models.⁶⁹

OR measurements were accelerated by lasers and photon counting technology in 1983 with the so-called high-accuracy universal polarimeter (HAUP) method^{70,71} whereby OR was extracted at a fixed wavelength as a function of motorized settings of a polariser and analyser. The HAUP method was a watershed in the history of chiroptics.⁷² The introduction of other variables into HAUP-like polarimeters such as the incident angle⁷³ or wavelength⁷⁴ improved the data fitting algorithms. Asahi and coworkers generalized HAUP for compatibility with spectrophotometers and the determination of dissipative effects of LD and CD in what was called generalized HAUP or G-HAUP.^{75,76,77,78} HAUP analyses continue in Tokyo and elsewhere.^{79,80,81}

With the aggregate approaches outlined above, CB (CD) could be measured in the presence of LB (LD). However, the list of crystals for which complete CB anisotropy has been determined grows at a rate of about 1/yr.^{82,83} Only a small number of organic compounds have been analysed in full. These include *L*-tartaric acid⁸⁴ and its salts.^{85,86} Benchmark measurements of a reduced sugar,⁸⁷ amino acids^{88,89} and lysozyme, the only biomolecule single crystal so analysed, were reported.⁹⁰ However, comparisons among this small set provides little predictability. For instance, *L*-tartaric acid has four independent tensor elements in the monoclinic system, $OR_{11} = 79(7)$ deg mm^{-1} , $OR_{22} = 90(13)$, $OR_{33} = -70(4)$, $OR_{23} = -18(8)$ rather than merely a specific rotation.⁸⁴ Without an intuitive way to interpret these values in terms of structure, an observer might presume we have labored to quadruple the values that we don't understand.

Infelicitous Linkage of Chirality and Optical Activity

Pasteur dissolved his transparent crystals of the sodium ammonium tartrate conglomerates and established by polarimetric analysis that *dissymetrie*, chirality, was the necessary condition for OA of molecules (in solution).^{91,92} Understandably, he overgeneralized his observations, unaware of the necessity of the parenthetical addition in the preceding sentence. For isotropic solutions only, chiral molecules are indeed requisite. However, Pasteur has been a beacon and we have differed as a community to his judgment. Popular textbooks have reinforced this linkage, such as that used by one of the authors (BK). According to Morrison and Boyd, "the same non-superimposibility of mirror images that gives rise to enantiomerism is also responsible for optical activity."⁹³ This is misleading. Only with a new generation of textbooks⁹⁴ can this linkage be fully broken.

For oriented, isolated molecules, or molecules lined-up as in single crystals, some non-enantiomorphous systems can be OA.^{95,96} Nevertheless, we had to wait generations before this could be demonstrated for one such direction of one such crystal, AgGaS₂.^{97,98} favored by an accidental isochrony (equivalence) in the refractivities in a low symmetry direction. The two characteristic polarisations of light propagating through the anisotropic crystal just happened to be degenerate at one wavelength and the LB disappeared. The azimuth of light rotated, and associated polarimetric intensity changes were easily measured and interpreted.

AgGaS₂ with point symmetry $\bar{4}2m$ (D_{2d}) or crystals in the non-enantiomorphous subgroups m (C_s), $\bar{4}$ (S_4), $mm2$ (C_{2v}) have finite elements ρ_{ij} but with traces of zero (diagonalized: $[\rho_{11}, 0, 0; 0, -\rho_{11}, 0; 0, 0, 0]$ in Matlab matrix format).⁹⁹ Molecules in these point groups will have a dextrorotatory direction (ρ_{11}), and an equal and opposite levorotatory direction ($\rho_{22} = -\rho_{11}$). Such molecules in solution will give specific rotations (average values) of zero, however *they are not optically inactive*. If oriented in a crystal of the same symmetry, a difference in interactions with left and right CP light is affected in most¹⁰⁰ directions. These facts were illustrated recently in achiral metal perovskites,¹⁰¹ but muddled elsewhere.¹⁰²

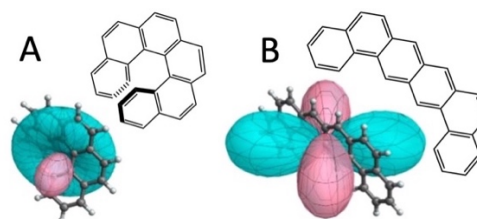


Figure 3. Representation surfaces plotted to same scale of the OR (computed at 630 nm) of C₂₆H₁₆ isomers. A. Chiral hexahelicene (left) and B. dibenzo[*a,h*]tetracene (right). Red = dextrorotation, green = levorotation. Copyright American Chemical Society, ref. 103.

Mason once taught, "The helicene series owe their optical activity principally to the inherently dissymmetric π -electron system."⁷ More accurately, only the non-zero spatial average owes a debt to dissymmetry. Flat oriented molecules are *more* OA than their helical isomers in some directions¹⁰³ as seen in the Figure 3 comparison of the OR anisotropy of hexahelicene and an achiral, C_{2v} constitutional isomer. The reason is simple. Electrons achieve a greater circulation and large moments in Eq. 5 if they stay in a plane as opposed to climbing a spiral staircase, so to speak. Helicenes are only special objects of chiroptical investigations because the spatial average of the OR tensors is non-zero and often large. While the higher symmetry of the C_{2v} isomer renders to dot product of transition and magnetic dipoles as zero, in oriented system the role of the wave vector in mixing these moments is essential.^{104,105}

We aspired to measure the long wavelength OR of isostructural crystalline (point group $\bar{4}2m$, D_{2d})¹⁰⁶ compounds MPh₄, where M = C, Si, Ge, Sn, and Pb, with a central, tetravalent carbon atom bonded to four chemically identical, simple (non-stereogenic) substituents. In organic chemistry pedagogy, such a compound (like pentaerythritol)¹⁰⁷ could hardly be more optically inactive. We aimed to show otherwise. In work of this kind, large, high-quality crystals necessitate cutting and polishing with the skill of a lapidary. The MPh₄ crystals were too soft (think of polishing a candle).

We turned to the hydrogen bonds of pentaerythritol $\bar{4}$ (S_4) to 'toughen-up' our surfaces¹⁰⁷ and measured the response by tilting the crystal in a HAUP-based apparatus.¹⁰⁸ Yet, in solution, pentaerythritol has a specific rotation of zero as opposed to being *optically inactive*. This is a subtle point. If pentaerythritol were centric it would be intrinsically optically inactive (all tensor elements would be zero – $[0,0,0; 0,0,0; 0,0,0]$ – and the polarimeter would

obviously deliver zero.⁵⁵ Here, we stress the general non-utility of the specific rotation, valued at zero for every OA *achiral* molecule, no matter the structure. Pentaerythritol and nonactin, both OA molecules with symmetry $\bar{4}$ (S_4) could not be distinguished from one another by solution polarimetry. Only the response of their crystals would embrace the great differences in the composition, configuration, and electronic structure. There remains a natural tendency to call molecules that fail to register in a solution polarimeter (cryptochirality¹⁰⁹ notwithstanding) optically inactive. This is a misconception that arises in the long-standing restriction of polarimetry to isotropic media.

Mueller's Polarisation Transformation Matrix

Theory

The polarisation of light propagating through a medium can be described by a Stokes vector, \mathbf{S} , a four-element column of real-valued polarisation state sums and differences. The analyte is represented by Mueller's 4x4 transformation matrix \mathbf{M} ^{110,111,112,113} that operates on \mathbf{S} . \mathbf{M} transforms one Stokes vector into another, $\mathbf{S}_{\text{out}} = \mathbf{M}\mathbf{S}_{\text{in}}$, and has been called "a model of the medium."¹¹⁴ Generally, we do not know the form of \mathbf{M} . Polarimetry aims to build and interpret this model.¹¹⁵ \mathbf{M} can be a matrix of numbers (Figure 4A), or a matrix of spectra as a function of some parameter like the wavelength (Figure 4B), or it can be a matrix of images (Figure 4C).

\mathbf{M} can be calculated from first electro-dynamical principles according to Berreman,^{116, 117, 118} and the results compared directly to experiment. To model OA along a general direction of a crystal one must understand how the constitutive tensors like the permittivity $\boldsymbol{\varepsilon}$, and the magneto-electric tensor $\boldsymbol{\alpha}$ above, affect the interactions of crystals with light.^{119,120} Such crystals are called bianisotropic.¹²¹ To date, we have not investigated the polarimetric properties of any magnetic materials and thus $\boldsymbol{\mu}$, the permeability, is taken as the identity matrix. $\boldsymbol{\varepsilon}$ and $\boldsymbol{\alpha}$ tensors are generally complex and determine the dispersive effects, LB and CB, as well as the dissipative effects, LD and CD, that are manifest in the output. The analysis begins with Maxwell's constitutive equations in matrix form (Eq. 7):

$$\begin{bmatrix} D \\ B \end{bmatrix} = \begin{bmatrix} \boldsymbol{\varepsilon} & -i\boldsymbol{\alpha} \\ i\boldsymbol{\alpha}^T & \boldsymbol{\mu} \end{bmatrix} \begin{bmatrix} E \\ H \end{bmatrix}. \quad (7)$$

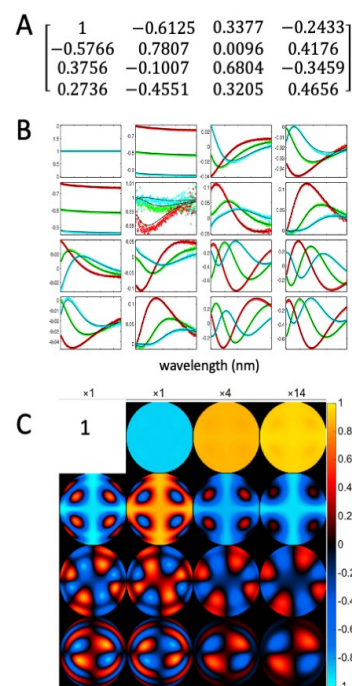


Figure 4. Mueller matrices. (A) Arbitrary \mathbf{M} (B) Comparison of the measured and fitted reflection \mathbf{M} s of ethylene diammonium sulfate (EDS, Figure 2A). Each of the three spectra sets represents \mathbf{M} measured at (red) 40°, (green) 45°, and (blue) 50° angles of incidence. Republished from ref. 152, with permission of Wiley-VCH. (C) k -space map of the fluorescence Mueller matrix of a (001) slice of a dyed crystal as in Figure 12A. Ref.200. Copyright S. M. Nichols, Dissertation, New York University, 2018.

Vectors D and B induced in a material are related to applied field vectors E and H by a 6×6 matrix composed of four 3×3 subtensors $\boldsymbol{\varepsilon}$, $\boldsymbol{\alpha}$, $\boldsymbol{\alpha}^T$, and $\boldsymbol{\mu}$. The evolution of the field vector components can be written as differential equation containing a matrix constructed from the constitutive tensor elements, parameters for fitting computation to experiment. The successive steps in computing and measuring the polarisation \mathbf{M} are given in Figure 5.

As polarised light traverses a homogeneous medium, the polarisation state will undergo a continuous evolution depending on the elementary polarisation properties (List 1).¹²²

List 1. Eight fundamental polarisation properties

Total Refractive Index	$\bar{n} = (n_0 + n_{90})$
Total Absorption	$\bar{\kappa} = (\kappa_0 + \kappa_{90})$
Horizontal Linear Birefringence	$LB = (n_0 - n_{90})$
Horizontal Linear Dichroism	$LD = (\kappa_0 - \kappa_{90})$
Diagonal Linear Birefringence	$LB' = (n_{45} - n_{-45})$
Diagonal Linear Dichroism	$LD' = (\kappa_{45} - \kappa_{-45})$
Circular Birefringence	$CB = (n_L - n_R)$
Circular Dichroism	$CD = (\kappa_L - \kappa_R)$

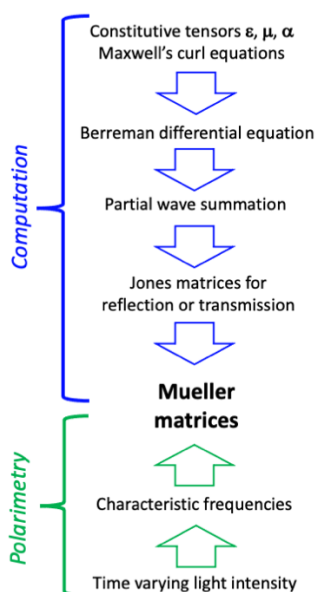


Figure 5. Flow chart for first electrodynamical-principles computation (blue top) and polarimetric measurement (green bottom) of \mathbf{M} . The tensor elements that are sought can be adjusted to best fit the experimental \mathbf{M} .

\mathbf{M} arises from the transformation of a Stokes vector, \mathbf{S} , over an infinitesimal length in a homogeneous medium: $d\mathbf{S}/dz = \mathbf{m}\mathbf{S}$, where \mathbf{m} is the differential Mueller matrix. Integrating yields:

$$\mathbf{S}_{\text{out}} = \exp\left(\int_0^z \mathbf{m} dz\right) \mathbf{S}_{\text{in}} = \exp(\mathbf{m}z) \mathbf{S}_{\text{in}} = \mathbf{M} \mathbf{S}_{\text{in}}, \text{ where} \quad (8)$$

$$\mathbf{m} = \begin{bmatrix} -\bar{\kappa} & -LD & -LD' & CD \\ -LD & -\bar{\kappa} & CB & LB' \\ -LD' & -CB & -\bar{\kappa} & -LB \\ CD & -LB' & LB & -\bar{\kappa} \end{bmatrix} \approx \begin{bmatrix} m_{11} & m_{12} & m_{13} & m_{14} \\ m_{21} & m_{22} & m_{23} & m_{24} \\ m_{31} & m_{32} & m_{33} & m_{34} \\ m_{41} & m_{42} & m_{43} & m_{44} \end{bmatrix}$$

The matrix logarithm of \mathbf{M} , is a numerical approximation of \mathbf{m} (eq. 8) that deconvolves linear and circular anisotropies, revealing each optical effect as a unique element in \mathbf{m} . The elements of \mathbf{m} can also be computed analytically.¹²³

Measurement

Mueller matrix polarimetry is in effect transmission ellipsometry, albeit reflection and transmission measurements are complementary.^{124, 125, 126} The \mathbf{M} formalism is mathematically robust,¹²⁷ and its elements are derived from light intensity measurements. The first Mueller polarimeter we constructed used rotating waveplates and a camera as the detector.^{128, 129, 130, 131, 132, 133} Here, polarisation modulation was slow, but imaging was fast. The

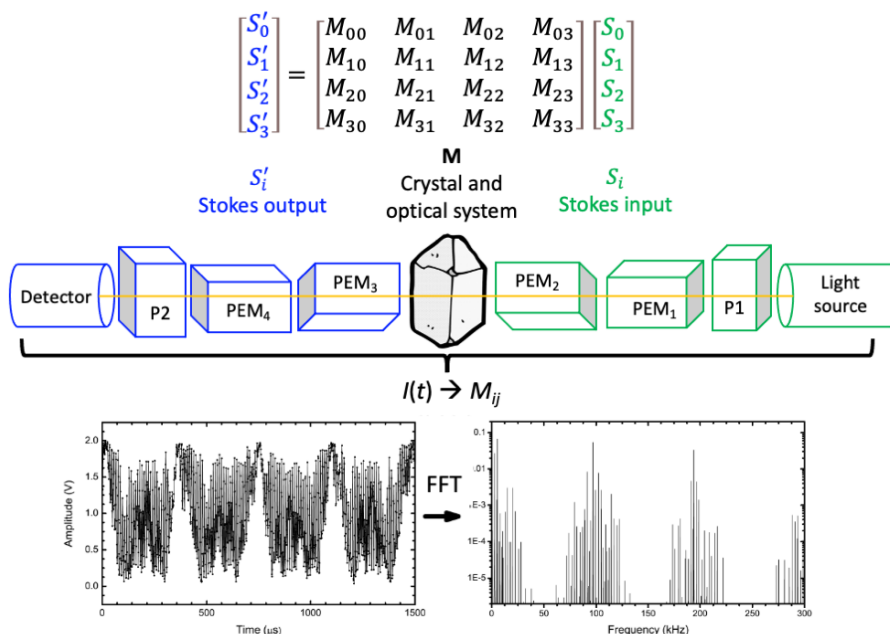


Figure 6. Schematic determination of the experimental \mathbf{M} using a 4-PEM polarimeter in transmission. (Top) Input Stokes vector (S_i) from a polarisation state generator is multiplied by \mathbf{M} of the sample and optical system to give an output Stokes vector (S'_i) after traversing a polarization state analyzer. Elements M_{ij} are constructed as integral sums and differences of frequencies extracted from the time varying intensity signal, $I(t)$, by Fourier analysis (FFT).

These properties are defined here as subscripts with respect to four directions, 0° , 90° , and $\pm 45^\circ$, as well as left (L) and right (R) CP light. Total refraction is given by \bar{n} , and extinction by $\bar{\kappa}$. The quantities in List 1 are unitless material characteristics. The literature frequently uses the same acronyms (LB , CB , LD , CD) for path length dependent quantities multiplied by the wave vector and the thickness. It is more accurate in such instances to refer to retardances and extinctions (LR , CR , LE , CE), extrinsic effects.

device was well suited to measurements of OA of small crystals along the optic axis. Mechanical instabilities thwarted measurements of CB and CD in low symmetry directions.

Arteaga and Jellison redetermined the OR anisotropy of α -quartz using photoelastic modulators (PEMs), instead of mechanically modulated polarisers. Commercial CD spectropolarimeters that are common in most chemistry departments invariably use a single PEM¹³⁴ delivering just 1/16 of \mathbf{M} . The quartz analyzers used two PEMs

operating at different frequencies that were reconfigured (reoriented in space) to extract from the time varying intensity the frequencies necessary to solve the four linear equations in Figure 6.¹³⁵ This demonstration directed our efforts with Arteaga toward of a transmission ellipsometer with four PEMs operating synchronously.¹³⁶ In this '4-PEM' configuration all 16 elements of **M** could be extracted without moving any optical component, a boon when looking for small contributions to the intensity.¹³⁷

Illustrations

The 4-PEM delivered the values expected for slabs of quartz, the perennial starting point for new efforts to evaluate the OA of crystals, parallel and perpendicular to the *c*-axis.¹³⁸ We returned to quartz with a more efficient approach to recover all the elements of ϵ and ρ from a single specimen.¹³⁹ One of the most time-consuming steps in the analysis of OA anisotropy single crystals is cutting and polishing plane parallel slabs for each independent tensor element investigated. However, save this labour, Nichols needed to reckon with the incoherencies of multiple reflections of a spectroscopic light source from comparatively thick specimens.^{140,141,142} The optics of moderately thick anisotropic layers as in lab-grown crystals assessed with light of comparatively short temporal coherence length (persistence of phase relationships) is challenging because outgoing rays differing in the number of internal reflections become incoherent as the accumulated optical path difference grows. Only very thin layers coalesce raylets into a coherent field described exactly by Berreman's method. We adopted a method for treating the summation of incoherent rays¹⁴³ having made multiple passes through an anisotropic crystal,¹⁴⁴ the so-called partial wave method.¹³⁹ AgGaS₂,^{97,98} the next most widely studied OA crystal, was likewise reinvestigated with the 4-PEM.^{136, 145}

Hippuric acid crystals (enantiomorphous, *P*₂*1*₂*1*₂) grow with helicoidal morphologies having potential chiroptical consequences.^{130, 146} However, they have large LB (0.23).¹⁴⁷ We ascribed to them a hypothetical α tensor; ϵ was known. The total retardance was then calculated for all directions by the Berreman method and then projected onto a hemisphere with and without the inclusion of α .¹⁴⁸ The only place where we could hope to find a measurable difference between the **M**s was along an optic axis, whereas in all other directions, the results were barely distinguishable, emphasizing the dominance of LB (the 'dark matter' in Figure 7).



Figure 7. Hemisphere upon which is projected the difference between the total retardance computed from the **M**s of hypothetical hippuric acid with a known ϵ and α . Ref. 148. Copyright J. F. Freudenthal, Dissertation, New York University, 2012, with permission.

Benzil was analysed by the 4-PEM and the partial wave method to deliver the ORD for all directions from a single slice.^{139,140,141} The same results were obtained collaboratively by the HAUP method and compared directly.¹⁴⁹



The OR¹⁵⁰ and ORD¹⁵¹ of chiral (*P*₄*1*₂*1*₂ and *P*₄*3*₂*1*₂) crystalline ethylene diammonium sulphate (EDS) had been determined. Large crystals (1 cm³) were grown from water with large facets normal to the [001] and with perfect cleavage.¹⁵² Ethylene diammonium selenate (EDSe) is isostructural (Figure 2A).¹⁵³ Dispersion relations for the ϵ and α elements of EDS were determined with the 4-PEM by measuring a plate at a variety of incidence angles and analysed using the partial wave method.¹⁵⁴ EDSe has a AgGaS₂-like isotropic point at 364 nm. At this wavelength, the dispersion curves of the ordinary and extraordinary refractive indices cross, and the medium becomes optically isotropic. The absence of parasitic linear anisotropies permits the recovery of OA,¹⁵⁵ even along general directions. Crystals of EDS grown in the presence of EDSe selectively incorporate selenate in the host crystal structure, disrupting the symmetry.^{156,157} This desymmetrisation creates evident LB in directions where it would otherwise be forbidden. By characterizing the composition of solid solutions, we connected how the OR of end members evolve as the additive concentration.¹⁵³

Another crystal with an isotropic point like EDSe or AgGaS₂, KTC (potassium trihydrogen di-(*cis*-4-cyclohexene-1,2-dicarboxylate) dihydrate),¹⁵⁸ was analysed likewise^{139,140,141,142} and a workflow is given in Figure 8 from molecular structure to dispersion of the tensor elements.

Interpretation in Molecules

Before tackling the interpretation of the OA of oriented crystals, we must address the interpretation of OA in oriented molecules. Capturing the CD anisotropy of single molecules has been equivocal.^{159,160,161,162} For this reason, the chiroptical anisotropy of single molecules remains a subject best investigated by computations. We surmised that an intuitive understanding of OR would first come from molecules for which we have an intuitive understanding of electronic structure. Unfortunately, as chemists, we do not have that understanding for many molecules. Wave functions for one OA H₂O molecule¹¹ can be quickly drawn on a chalkboard by most chemists¹⁶³ whereas approximations (cartoons) of the wave functions of H₂O₂ in its chiral, skew-symmetric ground state, a typical starting point for theoretical considerations of OR,^{164, 165, 166, 167} would be comparatively challenging. After approximating the excited states as one electron excitations it is relatively to 'see' where the OA arises. Unfortunately, it would be beyond the scope of contemporary science to measure the CB of one oriented water molecule, albeit some rare phases of ice crystallise in OA point groups.¹⁶⁸ Moreover, water does not take us far into organic chemistry.

On the other hand, π wave functions of planar conjugated hydrocarbons, can be estimated by inspection from the knowledge of the normal modes of a guitar string, or derived by back-of-the-envelope Hückel theory.¹⁶⁹ The separability of σ and π orbitals has been a powerful simplifying idea in organic chemistry and provides us with a large class of important molecules for which part of the electronic structure is intuitive. In fact, for $mm2$ (C_{2v})-symmetric dienes, trienes, tetraenes, and pentaenes that behave like bent wires, one can come within $\pm 20\%$ of the non-resonant OA by only

several percent of the response and can be neglected for pedagogical purposes.^{169,170,171} With these simplifications through the thickets of electronic structure for a class of compounds that are at the heart of organic chemistry, the anisotropy of OA can be explained with freshman physics (dipole scattering) (Figure 10E).^{171, 172} The product of cartoons of the HOMO and LUMO gives the overlap density (Figure 10C,D) and the transition dipole moments. Dipole scattering produces a component of the electric field that is polarized perpendicular to the driving field and in phase with it.

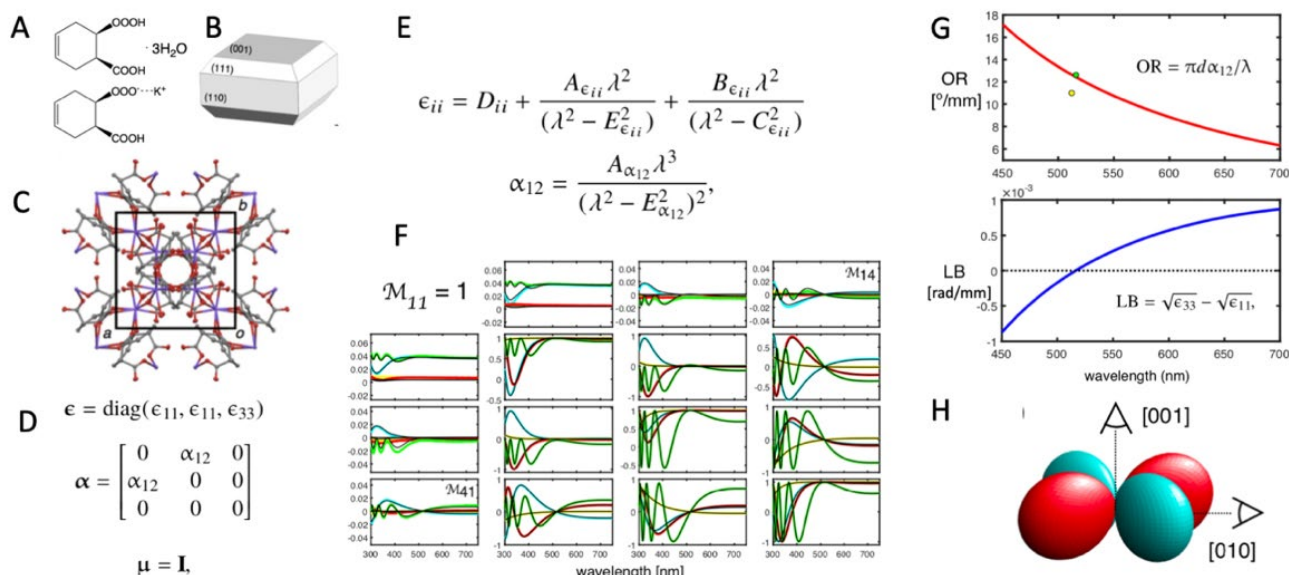


Figure 8. Workflow for ϵ and α of KTC (see text). A. KTC structural formula. B. Idealized crystal habit place (plotted with the software WinXMorph software (<http://cad4.cpac.washington.edu/WinXMorphHome/WinXMorph.htm>)). Crystal viewed down c . D. Constitutive tensors for symmetry $42m$. E. Phenomenological dispersion relations. F. Angle and wavelength dependent normalized Ms from experiment. Dispersion plotted for OR and LR (labeled as LB). Green dot is previously established from the literature. G. Representation surface of OR (deg mm^{-1}). Assembled from ref. 158, with permission of Wiley-VCH.

considering the contribution of the B_1 HOMO (a_2) \rightarrow LUMO (b_2) excitation, obviating sums over hundreds of excited states⁵⁴ and focusing on a single state such that $\rho_{ij} \propto R_{ij}^{HOMO \rightarrow LUMO}$ (Figure 9A,B). The overwhelming importance of the first excited state dominated by the HOMO \rightarrow LUMO excitation is shown in a sum-over-states convergence plot with and without the first excited states of long wavelength OR compared with linear response theory (Figure 9A).¹⁷⁰

For conjugated hydrocarbons, only m and μ are important, the electric dipole-electric quadrupole contributions account for just

At this point, we can begin to distinguish the OR of molecules based on their predominant resonance structures, or on the degree of their aromaticity^{171, 173} (Figure 9B). In other words, we can make interpretations in terms of the organic model which imputes physical and chemical properties to Lewis structures.

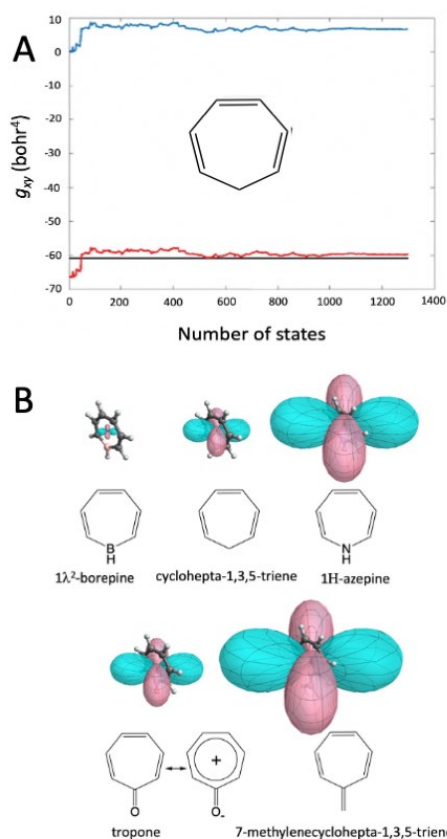


Figure 9. A. Sum-over-states of rotatory strength tensor elements in the xy direction, expressed as the cumulative gyration tensor¹ element $g_{xy} \propto \rho_{ij}$, in atomic units of bohr⁴/molecule. Solid black line is value for g_{xy} computed at 630 nm by the linear response DFT method. The red line is the sum-over-states values. Ref. 170. Copyright V. L. Murphy, Dissertation, New York University, 2015. The blue line represents the summation that begins with S_2 , the second excited state that reflects the HOMO-LUMO excitation. B. Representation surfaces of the OR anisotropy of cycloheptatrienoids. Antiaromatic molecules are more active than aromatic molecules because the circulation of charge is in-phase with an in-plane transition electric dipole. Likewise, aromatic resonance structures are less responsive compared to those that do not. Reprinted from ref. 215 with permission of the American Chemical Society.

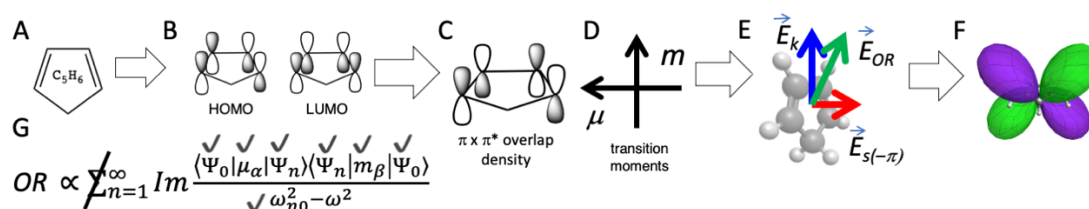


Figure 10. From a single, oriented molecule to chiroptical anisotropy. A. Structural formula. B. HOMO and LUMO. C. Overlap density and D. associated transition electric (μ) and magnetic (m) dipole moments. E. Electric dipole scattering E_s (red) from induced moments out of phase ($-\pi$) with the driving field E_k (blue) to give E_{OR} (green). F. Representation surface of the chiroptical anisotropy. G. Rosenfeld formula (ref. 172) simplified for compounds like cyclopentadiene by obviating the sum over states. Ground state and first excited state are intuitive. The resonance frequency can be estimated from experience. From ref. XX with permission of the American Chemical Society

Crystals

No general, first principles quantum chemical method^{174, 175} for computing the OR of crystals has been implemented in widely available electronic structure computing programs.¹⁷⁶ Linear response theories with periodic boundary conditions are required because OA of molecules is strongly effected by environment as confirmed by experimental and computational studies on the solvent dependence of OR,¹⁷⁷ in addition to many studies of

computational investigations of crystallographic supercells that we can carried out over the years. To minimize the effects of interfacial molecules, larger and larger aggregates of molecules must be computed, a process that becomes intractable. Baldud and Caricato made this convergence problem in one-dimension explicit for diatomic molecules (e.g. F_2 and HF) arranged as model supramolecular helices. Unit cells were inadequate representations of large helices underscoring the necessity of implementing periodic boundary conditions. [As this paper was to be posted online, a new publication announced computed results of the chiroptical

properties of periodic systems: on the self-consistent coupled-perturbed method in CRYSTALS was adopted to periodic systems, such as quartz, tartaric acid crystals, and carbon nanotubes.¹⁷⁸

An alternative approach would follow our analysis of conjugated hydrocarbons: Build crystals from molecules with large chiroptical responses that can be reckoned from qualitative molecular orbital theory. Treat the supramolecular interactions as a perturbation of the primary, additive response of oriented molecules. The analysis of the OA anisotropy for simple conjugated hydrocarbons would be extremely challenging to match with chiroptical measurements of cyclopentadiene (m.p. -90 °C) or cycloheptatriene (m.p. -80 °C) single crystals. However, there is a large class of molecules with the requisite characteristics, the BODIPY (BORon DIPYromethene)^{179,180} luminophores. The parent compound is U-shaped, *mm2* (C_{2v}) symmetry with 12- π electrons (Figure 11A,B). The HOMO and LUMO can be approximated by inspection. From the overlap density, the relative phases of the μ and m (Figure 11C) are sufficient for predicting the anisotropy of the OR or CD. Of the ca. 400 BODIPY crystal structures currently deposited in the Cambridge Structural Database at the time of publication, 12% are optically active.

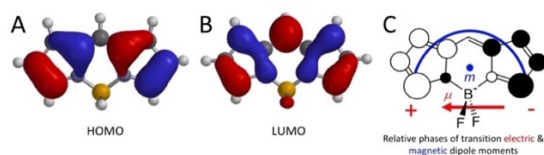


Figure 11. Orbitals to anisotropy. A. BODIPY HOMO, B. LUMO, C. Overlap density and determination of transition μ and m . It is trivial to 'compute' the overlap density from where the moments arise in the mind's eye because the planar molecule has flat wave functions. We can reckon CD anisotropy from projections of the respective transition moments onto the wave vectors as in Figure 10.

Outlook

Data Analysis

Speeding up the process of the reliable determination of the OA of single crystals required several interventions. Firstly, the development of a polarimeter (4-PEM)¹³⁶ that could deliver the \mathbf{M} without mechanically reconfiguring any optical components. Secondly, routine operation in non-normal incidence, thereby reducing the number of different plane parallel polished crystal sections; this required reckoning with incoherencies in multiple reflections.^{140,142} At present, fitting \mathbf{M} calculated by the partial wave method, operating from the constitutive tensors, is the slowest step. For an orthorhombic, absorbing, OA crystal, for example, there will be twelve independent components of the complex tensor elements, and more for lower symmetry crystals.

Nowadays, actively fitting data with iterative least squares algorithms is losing ground to advances in machine learning. Martin explored support vector machines¹⁸¹ for fitting experimental \mathbf{M} s to give dispersion relations of tensorial parameters straightaway.⁸³ With the Berreman and partial wave methods we computed ca. 10^5 random Mueller matrices in transmission at a variety of incidence angles for chiral and uniaxial crystals like quartz, but with a range of arbitrary values for the permittivity (ϵ_{11} , ϵ_{33}), magnetoelectric (α_{11} ,

α_{33}) tensors. Then the algorithm guessed the dispersion relations for \mathbf{M} s for a crystal with actual tensor values. Given the pace at which machine learning is making in-roads into all aspects of science, a general algorithm for fitting \mathbf{M} s may be in reach.

Conoscopy and Fluorescence

The 4-PEM polarimeter has been used to make images, either by scanning a pinhole^{137,182} or by using stroboscopic light sources that illuminate a sample at the frequencies that are needed to construct \mathbf{M} .¹⁸³ Alternatively, an optical microscope

can be fashioned in Mueller matrix imaging systems with CCD or CMOS camera detectors. Light modulation is accomplished with continuously rotating waveplates^{184, 185} in lieu of PEMs. Optical microscopes can in principle image the front or back focal plane of the objective. In the former case, space is resolved directly (orthoscopic illumination) whereas in the latter case the image is composed of wave vectors (conoscopic illumination),¹⁸⁶ a standard technique in crystal optics as in Figure 3C, which also illustrates that emitted light can also be brought within the framework of Mueller matrix analysis.^{187, 188, 189, 190, 191} The fluorescence Mueller matrix connects the Stokes vector at the excitation wavelength to the outgoing Stokes vector at the emission wavelength. This work grew from efforts to evaluate the CD anisotropy^{192,193,194,195,196,197} of dyed crystals,^{83,198,199} for instance Figure 12.^{140,200}

Transparent, uniaxial crystals with isotropic points are particularly attractive because they provide a strategy for determining the CD anisotropy of molecules oriented and overgrown by the crystalline hosts. KTC grown in the presence of cresyl violet meets these conditions.⁸³ Computed CD anisotropy of oriented dyes were reported recently.^{57,58}

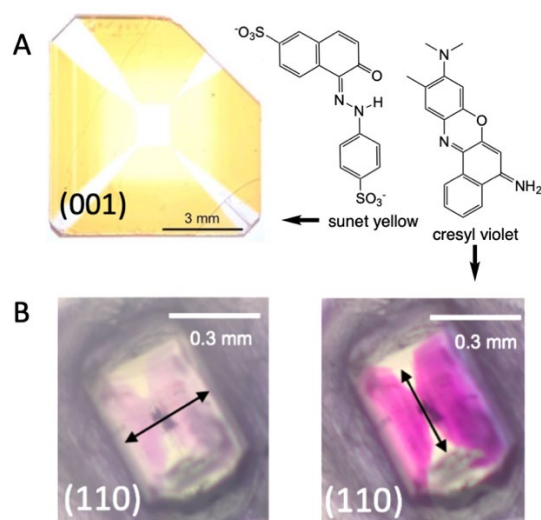


Figure 12. (A) An (001) slice of an EDS crystal grown from solution containing the azo dye sunset yellow. (B) KTC crystal as grown with cresyl violet in light polarized parallel and perpendicular (black arrows) to the optic axis (elongated direction).

Polycrystalline Structures

We can analyze the differential transmission of left and right CP light in highly structured polycrystalline materials using Mueller matrix

microscopy. The CB measured in these instances does not arise in natural OA, a consequence of the dissymmetry of polarisable groups within a molecule²⁰¹ or single crystal. Rather, it stems from the dissymmetry of micron-size anisotropic substructures with respect to one another.^{202,203,204,205,206,207}

A vivid example maps the sense of splay of anisotropic lamellae in spherulites of polycrystalline aspirin grown from the melt in Figure 13. Circular retardance is non-zero even though aspirin is centrosymmetric and cannot have natural OA. The etiology of the sensitivity to CP light arises in the bisection of a spherulite into halves that are, respectively, dextrorotatory and levorotatory. Aspirin lamellae splay by small angle branching of a nucleus with $2/m$ (C_{2h}) symmetry with a positive sense (right-handed) for one $\langle 010 \rangle$ direction and with a negative sense for the opposite direction.²⁰²

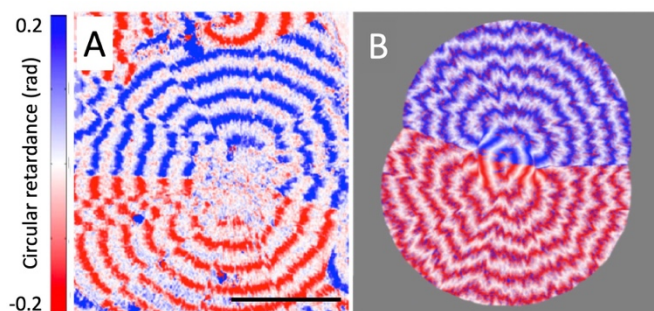


Figure 13. Comparison of (A) experimentally measured circular retardance image of banded aspirin spherulites (scale bar = 250 nm) and (B) phase field simulation from ref. 208. Part B Copyright American Physical Society.

Beyond Molecules, Visible Light, and Circular Polarization

Nanofabricated metallic structures have spatial dimensions on the order of the wavelength of light with highly polarisable electrons (plasmons).²⁰⁹ The helical configuration of the electric field in CP light spills across the structure. The CR and CE of such structures can be comparable to the LR and LE. In fact, a helicoidal gold needle on the order of 1 μm will easily discriminate between the sense of CP light.^{210,211,212}

Vibrational optical activity, that is vibrational circular dichroism (VCD) and Raman optical activity (ROA), are weaker than corresponding electronic processes.^{8,213} However, these techniques have advanced markedly, and researchers are now framing the problems of anisotropy in VCD²¹⁴ and ROA.²¹⁵

Lastly, we emphasize that chemists have for two centuries struggled to make molecules and superstructures more responsive – we dare not say *more* dissymmetric – to CP light.²¹⁶ An exciting alternative is to make light more twisted than mere circular polarisation. So-called superchiral light^{217,218} that can arise in the near-field of plasmonic particles²¹⁹ promises to flip our perspective on light-matter interactions that could not have been foreseen at the start of the science of crystal chiroptics.^{17,20}

Conclusion

Reasons for developing more effective strategies for determining the OA anisotropy of single crystals follow: 1. Isotropic solutions give only average values for molecules rapidly, randomly reorienting and average values of bisignate quantities thwart structure property relations; 2. Whole classes of molecules – those in non-enantiomorphous point groups consistent with OA – can only have measurable values when fixed with respect to the wave vector of light. That is, the average value of OA for molecules of certain symmetries, irrespective of composition or structure, is a non-discriminating zero; 3. The aforementioned computations on achiral molecules simplify wave functions, facilitate structure-activity comparisons, and clarify the necessary and sufficient conditions for OA which is frequently misstated; 4. *Because it is there*. The difficulty of making chiroptical measurements on single crystals has confronted scientists for more than 200 years. It is a challenge that has overstayed its welcome.

Conflicts of interest

There are no conflicts to declare.

Acknowledgements

This work was primarily supported by the US National Science Foundation ((DGE-12342536, DMR-1105000) and the US National Institutes of Health (5R21GM107774-02) as well as the New York University Department of Chemistry Kramer and Sokol fellowship programs. Figures of tensors centered on molecules were drawn with a program courtesy of Professor J. Autschbach (University of Buffalo). BK thanks Professors W. Kaminsky (University of Washington), O. Arteaga (University of Barcelona), and A. G. Shtukenberg (New York University) for many important lessons. Thanks are additionally extended to Drs. K. Claborn, John Freudenthal, X. Cui, for their PhD theses of 2007, 2012, and 2015, respectively.

COMMUNICATION

Alex Martin was born in Pennsylvania in 1991. He studied physical chemistry at Boston College (BS) and New York University (Ph.D., 2018). He then moved into climate and energy policy, completing post doctoral fellowships at the National Academies of Sciences, Engineering, and Medicine and in the U.S. Congress where he staffed Senator Brian Schatz (D-HI). He now works on climate finance policy at Americans for Financial Reform, a DC-based think tank.



Shane Nichols was born in Alaska in 1988. He studied chemistry at Kansas State University (BS) and New York University (Ph.D., 2018). He did a postdoc at Harvard University in a neuroscience group before joining the senior staff at the Johns Hopkins University Applied Physics Laboratory in the Optics and Photonics Group, where he works on a variety of government programs.



Veronica L. Murphy was born in New Jersey in 1986. She studied chemistry at William Paterson University of New Jersey (BS, 2009) and New York University (PhD, 2016). She did her postdoc with NYU's College of Core Curriculum (2016-2018) teaching introductory chemistry to non-science majors. She is currently teaching Advanced Placement calculus and chemistry at Bethlehem Catholic High School and is pursuing a Masters in Secondary Education through Cedar Crest College. She plans to transition into a public-school teaching career at the high school Advanced Placement level, preparing college-bound students for the rigors and structure of college level courses.



Bart Kahr was born in NYC in 1961. He studied at Middlebury College, Princeton University (Ph.D., 1988), and Yale University. He was a faculty member at Purdue University from 1990-1996 and at the University of Washington, Seattle from 1997-2009. He returned to his hometown where he is currently Professor of Chemistry in the Molecular Design Institute at New York University. His research group studies the growth, structure, and physical properties of crystalline, an complex materials with a particular emphasis on new methods of metrology with polarized light, and the interpretation of the interactions of light with organized media.



Notes and references

- 1 J. Tyndall, *Faraday as a Discoverer*, D. Appleton and Company, New York, 1874; p.79, originally published in *Proc. Roy. Inst. Great Brit.* 1866-1869, **V**, 199–272.
- 2 B. Kahr, C. Isborn and K. Claborn, *Symmetry: Culture and Science*, **2005**, **16**, 423–429.
- 3 J.-B. Biot, *Mém. Acad. Sci.* 1835, **13**, 39–175.
- 4 B. Kahr, *International Union of Crystallography Newsletter*, 2002, **10**, https://www.iucr.org/news/newsletter/etc/legacy-articles?issue=20411&result_138864_result_page=12.
- 5 J.-B. Biot, *Bull. Soc. Philomat.* 1815, 190–192.
- 6 T. M. Lowry, *Optical Rotatory Power*, Longmans, London, 1935.
- 7 S. Mason, *Molecular OA and the Chiral Discriminations*, Cambridge University Press, Cambridge, 1982.
- 8 P. Polavarapu, *Chiroptical Spectroscopy. Fundamentals and Applications*, CRC Press, Washington DC, 2016.
- 9 P. Crabbé, *Optical Rotatory Dispersion and Circular Dichroism in Organic Chemistry, Holden-Day Series in Physical Techniques in Chemistry*. Holden-Day, San Francisco, CA, 1965.
- 10 D. A. Lightner and J. E. Gurst. *Organic Conformational Analysis and Stereochemistry from Circular Dichroism Spectroscopy*. New York, NY: Wiley-VCH, 2000.
- 11 L. D. Barron, *Molecular Light Scattering and OA*, 2nd ed. Cambridge, UK: Cambridge University Press. 2004.
- 12 J. Schellman and H. P. Jensen, *Chem. Rev.* 1987, **87**, 1359–1399.
- 13 J. Michl and E. W. Thulstrup, *Spectroscopy with Polarized Light*, Wiley-VCH, Weinheim, 1995.
- 14 H.-G. Kuball, *Chirality*, 2000, **12**, 278–286.
- 15 B. Kahr and R. W. Gurney, *Chem. Rev.* 2001, **101**, 893–951
- 16 B. Nordén, A. Rodger and T. Dafforn, *Linear Dichroism and Circular Dichroism*, RSC Publishing, Cambridge, 2010.
- 17 F. Arago, *Mém. Inst. Fr.* 1811, **1**, 93–134.
- 18 J. K. O'Loane, *Chem. Rev.* 1980, **80**, 41–61.
- 19 J. Applequist, *Am. Sci.* 1987, **75**, 59–68.
- 20 B. Kahr and O. Arteaga, *Chemphyschem*, 2012, **13**, 79–88.
- 21 L. Kristjánsson, Iceland spar and its influence on the development of science and technology in the period 1780-1930. 5th Ed. Manuscript courtesy of Kristjan Leosson, November 2020.
- 22 J. M. Adams and R. W. Small, *Acta Crystallogr. Sect. B*, 1974, **B30**, 2191-2193.
- 23 V. M. Agronovitch and V. L. Ginzburg, *Spatial Dispersion in Crystal Optics and the Theory of Excitons*, Interscience Publishers, London, 1966.
- 24 G. Szivessy and C. Münster, *C. Ann. Phys.* 1934, **20**, 703–736.
- 25 J. Kobayashi, T. Asahi, S. Takahashi and A. M. Glazer, *J. Appl. Crystallogr.* 1988, **21**, 479–484.
- 26 O. Arteaga, A. Canillas and G. E. Jellison, Jr. *Appl. Opt.* 2009, **48**, 5307–5317.
- 27 A. V. Shubnikov, *Principles of Optical Crystallography*, Consultants Bureau, Moscow, 1960.
- 28 R. Ossikovski and O. Arteaga, *Opt. Lett.* 2017, **42**, 3690–3693.
- 29 M. Born, *Optik*, Springer-Verlag. Berlin, 1930.
- 30 V. Devarajan and A. M. Glazer, *Acta Cryst.* 1986, **A42**, 560–569.
- 31 A. M. Glazer, *J. Appl. Crystallogr.* 2002, **35**, 652–652.
- 32 L. Rosenfeld, *Z. Phys.* 1928, **52**, 161-XX.
- 33 A. D. Buckingham, P. J. Stiles, *Acc. Chem. Res.* 1974, **7**, 258–264.
- 34 A. M. Glazer and K. Stadnicka, *J. Appl. Cryst.* 1986, **19**, 108–122.
- 35 K. Claborn and B. Kahr, W. Kaminsky, *CrystEngComm*, 2002, 252–256.
- 36 M. Pecul and K. Ruud, *Advances in Quantum Chemistry*; Elsevier: San Diego, 2005; pp 185–212.
- 37 T. D. Crawford, M. C. Tam and M. L. Abrams, *J. Phys. Chem. A* 2007, **111**, 12057–12068.
- 38 T. D. Crawford, *Theor. Chem. Acta.* 2006, **115**, 227–245.
- 39 P. L. Polavarapu, *Chem. Rec.* 2007, **7**, 125–136.
- 40 J. Autschbach, *Chirality* 2010, **21**, E116–E152.
- 41 J. Autschbach, *Top. Curr. Chem.* 2011, **298**, 1-98.
- 42 T. B. Pedersen, in *Handbook of Computational Chemistry* (J. Leszczynski, ed.) Springer, Dordrecht, 2012.
- 43 P. Polavarapu and C. Zhao, *Chem. Phys. Lett.* 1997, **296**, 105-110.
- 44 P. J. Stephens, D. M. McCann, J. R. Cheeseman and M. J. Frisch, *Chirality* 2005, **17**, S52-S64.
- 45 M. Krykunov and J. Autschbach, *J. Chem. Phys.* 2006, **125**, 034102–10.
- 46 B. Moore, M. Srebro and J. Autschbach, *J. Chem. Theory Comput.* 2012, **8**, 4336–4346.
- 47 H.-G. Kuball, T. Karstens, and A. Schönhofer – *Chem. Phys.* 1976, **12**, 1-13.
- 48 H. -G. Kuball and T. Höfer, in *Chirality in Liquid Crystals*, (H.-S. Kitzerow and C. Bahr, eds.) Springer-Verlag, Berlin, 2001; pp.67-100.
- 49 H.-G. Kuball, *Enantiomer*, 2002, **7**, 197-205.
- 50 H.-G. Kuball, E. Dorr, T. Höfer, and O. Türk, *Monat. Chem.* 2005, **136**, 289-324.
- 51 J. Autschbach, *ChemPhysChem* 2011, **12**, 3224-3235.
- 52 E. Charney, *The Molecular Basis of Optical Activity: Optical Rotatory Dispersion and Circular Dichroism*, John Wiley and Sons, New York, 1985.
- 53 M. Klessinger and J. Michl *Excited States and Photochemistry of Organic Molecules*, Wiley-VCH, Hoboken, NJ, 1995.

- 54 K. B. Wiberg, Y.-G. Wang, S. M. Wilson, P. H. Vaccaro and J. Cheeseman, *J. Phys. Chem. A* 2006, **100**, 13995-14002.
- 55 K. Claborn, Ph.D. Dissertation, University of Washington, Seattle, WA, 2006.
- 56 M. D. Kunrat and J. Autschbach, *J. Am. Chem. Soc.* 2008, **130**, 4404-4414.
- 57 M. Wakabayashi, S. Yokojima, T. Fukaminato, K. Shiino, M. Irie and S. Nakamura, *J. Phys. Chem. A*, 2014, **118**, 5046-5057.
- 58 M. Wakabayashi, S. Yokojima, T. Fukaminato, H. Ohtani, and S. Nakamura, *J. Chem. Phys.* 2015, **142**, 154102.
- 59 F. I. Fedorov, *Teorija girotropii*, Minsk: Nauka i Technika, 1976. [In Russian].
- 60 L. M. Barkovskii and G. N. Borzdov, in *Advances in Complex Electromagnetic Materials, NATO ASI Series*, (A. Priou, A. Sihvola, S. Tretyakov and A. Vinogradov, eds.) Springer Science + Business Media, Dordrecht, 1997.
- 61 A.F. Konstantinova, A. Yu. Tonin and B. V. Nabatov, in *Advances in Complex Electromagnetic Materials, NATO ASI Series*, (A. Priou, A. Sihvola, S. Tretyakov and A. Vinogradov, eds.) Springer Science + Business Media, Dordrecht, 1997.
- 62 B. N. Grechusshnikov and A. F. Konstantinova, *Comput. Math Applic.* 1988, **16**, 637-655.
- 63 A. F. Konstantinova and E. A. Evdischenko, *Proc. SPIE*, 1997, **3094**, 159-168.
- 64 O.A.Baturina, B.Brzezina, P.Bogachek, Z.B.Perekalina and A.F.Konstantinova, *Sov. Phys. Crystallogr.* 1987, **32**, 847-849.
- 65 B. N. Grechushnikov, A.F. Konstantinova, I.D. Lomako and I.N.Kalinkina, *Sov. Phys. Crystallogr.* 1980, **25**, 346-348.
- 66 A. I. Okorochkov, A. F. Konstantinova and Z. B. Perekalina, *Sov. Phys. Crystallogr.* 1983, **28**, 436-438.
- 67 A. I. Okorochkov, A. F. Konstantinova, L. V. Soboleva and L.I.Khapaeva, *Sov. Phys. Crystallogr.* 1985, **30**, 347-348.
- 68 N. R. Ivanov and A. F. Konstantinova, *Kristallografiya*, 1970, **15**, 490-499.
- 69 A. F. Konstantinova, T. G. Golovina, B. V. Nabatov, A. P. Dudka and B. V. Mill, *Crystallogr. Rep.* 2015, **60**, 907-914.
- 70 J. Kobayashi and Y. Uesu, *J. Appl. Crystallogr.* 1983, **16**, 204-211.
- 71 J. Kobayashi, Y. Uesu and H. Takehara, *J. Appl. Crystallogr.* 1983, **16**, 212-219.
- 72 A. M. Glazer, in *Physical Properties and Thermodynamic Behaviour of Minerals*, E. K. H. Salje (ed.), D. Reidel Publishing Company, 1988, 185-212.
- 73 W. Kaminsky and A. M. Glazer, *Ferroelectrics*, 1996, **183**, 133-141.
- 74 J. R. L. Moxon and A. R. Renshaw, *J. Phys.: Condens. Matter*, 1990, **2**, 6807-6836.
- 75 R. Matsuki, T. Asahi, J. Kobayashi and H. Asahi, *Chirality* 2004, **16**, 286-293.
- 76 J. Kobayashi and T. Asahi, *Proc. SPIE*, 2000, **4097**, 25-39.
- 77 A. Takanahe, M. Tanaka, K. Johmoto, H. Uekusa, T. Mori, H. Koshima, and T. Asahi, *J. Am. Chem. Soc.* **2016**, **138**, 15066-15077.
- 78 K. Nakagawa, and T. Asahi, *Sci Rep.* 2019, **9**, 18453.
- 79 M. Shopa, N. Ftomyn, and Y. Shopa, *J. Opt. Soc. Am. A*, **2017**, **34**, 943-948.
- 80 M. Shopa and N. Ftomyn, *Opt. Eng.* **2018**, **57**, 034101.
- 81 M. Shopa, and N. Fromyn, *J. Opt. Soc. Am.* 2019, **36**, 485-491.
- 82 W. Kaminsky, *Rep. Prog. Phys.* 2000, **63**, 1575-1640.
- 83 A. T. Martin, PhD dissertation, New York University, 2018.
- 84 D. Mucha, K. Stadnicka, W. Kaminsky and A. M. Glazer, *J. Phys.: Condens. Matter*, 1997, **9**, 10829-10842.
- 85 R. J. Lingard Dissertation, University of Oxford, 1994.
- 86 K. Saito, C. Fu-Tian and J. Kobayashi, *Japan. J. Appl. Phys.* 1992, **31**, 3225-3228.
- 87 W. Kaminsky and A. M. Glazer, *Zeit. Kristallogr.* 1997, **212**, 283-296.
- 88 T. Asahi, H. Utsumi, Y. Itagaki, I. Kagomiya and J. Kobayashi, *Acta Crystallogr.* 1996, **A52**, 766-769.
- 89 T. Asahi, M. Takahashi and J. Kobayashi, *Acta Crystallogr.* 1997, **A53**, 763-771
- 90 J. Kobayashi, T. Asahi and M. Sakurai, *M. Acta Crystallogr. Sect. A.* 1998, **A54**, 581-590.
- 91 L. Pasteur, *C. R. Séances Acad. Sci.* 1848, **26**, 535-538.
- 92 L. Pasteur, *Ann. Chim. Phys.* 1848, **24**, 442-459.
- 93 R. T. Morrison, R. N. Boyd, *Organic Chemistry*, 3rd Edition, Allyn and Bacon, Boston, 1973, p. 123.
- 94 W. H. Brown, B. L. Iverson, E. V. Anslyn, C. S. Foote, *Organic Chemistry*, 7th Edition, Brooks Cole, Belmont CA, 2014.
- 95 J. W. Gibbs, *Am. J. Sci.* 1882, **23**, 460 - 476.
- 96 W. Voigt, *Ann. Phys.* 1905, **18**, 645 - 694.
- 97 M. V. Hobden, *Nature*, 1967, **216**, 678.
- 98 M. V. Hobden, *Acta Crystallogr. Sect. A*, 1968, **24**, 676 - 680.
- 99 MathWorks[®], mathworks.com.
- 100 B. Kahr, A. T. Martin and K.-H. Ernst, *Chirality*, **2018**, **30**, 378-382.
- 101 P. C. Sercel, Z. V. Vardeny, A. L. Efros, *Circular dichroism in non-chiral metal halide perovskites, Nanoscale*, 2020, **12**, 18607.
- 102 L.-L. Xu, H.-F. Zhang, M. Li, S. W. Ng, J.-H. Feng, J.-G. Mao, D. Li, *J. Am. Chem. Soc.* 2018, **140**, 11569-11572.
- 103 V. L. Murphy and B. Kahr, *J. Am. Chem. Soc.* 2011, **113**, 12918-12921.
- 104 A. D. Buckingham, M. B. Dunn, *J. Chem. Soc. (A)*, 1971- 1988-1991.
- 105 O. Arteaga, *J. Opt.* 2014, **16**, 125707.
- 106 K. Claborn, B. Kahr and W. Kaminsky, *CrystEngComm*, 2002, 252-256.
- 107 K. Claborn, J. H. Cedres, C. Isborn, A. Zozulya, E. Weckert, W. Kaminsky and B. Kahr, *J. Am. Chem. Soc.* 2006, **128**, 14746-14747.

- 108 W. Kaminsky and A. M. Glazer, *Ferroelectrics*, 1996, **183**, 133–141.
- 109 K. Mislow, P. Bickart, *Isr. J. Chem.* 1976, **15**, 1–6.
- 110 H. Mueller, Report No. 2 of the OSRD project OEMsr-576, Nov. 15, 1943.
- 111 K. Järrendahl and B. Kahr, *Woollam Newsletter*, February 2011, pp. 8–9.
- 112 O. Arteaga, *J. Opt. Soc. Am. A*, 2017, **34**, 410+.
- 113 O. Arteaga, S. Nichols and B. Kahr, *Opt. Lett.* 2012, **37**, 2835–2837.
- 114 S. N. Savenko, in *Light Scattering Reviews 4* (A. A. Kokhanovsky, ed.) Springer, Berlin, 2009; pp. 71–120.
- 115 J. J. Gil and R. Ossikovski, *Polarized Light and the Mueller Matrix Approach*, CRC Press, Boca Raton, FL, 2016.
- 116 D. W. Berreman, *J. Opt. Soc. Am.* 1972, **62**, 502–507.
- 117 T. Scharf, *Polarised Light in Liquid Crystals and Polymers*, Wiley, Hoboken NJ, 2007.
- 118 R. M. A. Azzam and N. M. Bashara, *Ellipsometry and Polarised Light*, North-Holland, Amsterdam, 1988.
- 119 A. F. Konstantinova, K. K. Konstantinov, B. V. Nabatov and E. A. Evdichchenko, *Crystallogr. Rep.* 2002, **47**, 645–652.
- 120 A. F. Konstantinova, B. V. Nabatov, E. A. Evdichchenko and K. K. Konstantinov, *Crystallogr. Rep.* 2002, **47**, 879–882.
- 121 O. B. Arteaga and B. Kahr, *J. Opt. Soc. Am. B*, **2019**, **36**, F72–F83.
- 122 W. Kaminsky, K. Claborn and B. Kahr, *Chem. Soc. Rev.* 2004, **33**, 514–525.
- 123 O. Arteaga and A. Canillas, *Opt. Lett.* 2010, **35**, 559–561.
- 124 H. Arwin and D. E. Aspnes, *Phys. Today*, 2009, **62**, 70–71.
- 125 D. E. Aspnes, *Thin Solid Films*, 2004, **455**, 3–13.
- 126 R. M. A. Azzam, *Thin Solid Films*, 2011, **519**, 2584–2588.
- 127 D. H. Goldstein, *Polarised Light*. 2nd ed. Marcel Dekker, New York, 2003.
- 128 J. Freudenthal and B. Kahr, *Chirality*, 2008, **20**, 973–977.
- 129 J. Freudenthal, E. Hollis and B. Kahr, *Chirality*, 2009, **21**, E20–E27.
- 130 A. G. Shtukenberg, J. Freudenthal and B. Kahr, *J. Am. Chem. Soc.* 2010, **132**, 9341–9349.
- 131 H.-M. Ye, J. Xu, J. Freudenthal and B. Kahr, *J. Am. Chem. Soc.* 2011, **133**, 13848–13851.
- 132 A. G. Shtukenberg, X. Cui, J. Freudenthal, E. Gunn, E. Camp and B. Kahr, *J. Am. Chem. Soc.* 2012, **134**, 6354–6364.
- 133 J. Freudenthal, Dissertation, New York University, 2011.
- 134 M. Grosjean and M. Legrand, *C. R. Acad. Sci. (Paris)*, 1960, **251**, 2150–2152.
- 135 G. E. Jellison, Jr. and F. A. Modine, *Appl. Opt.* 1997, **36**, 8184–8189; 8190–8198.
- 136 O. Arteaga, J. Freudenthal, B. Wang and B. Kahr, *Appl. Opt.* 2012, **51**, 6805–6817.
- 137 O. Arteaga, J. Freudenthal, B. Wang, S. Nichols and B. Kahr, *Chimica Oggi (Chemistry Today)* **2012**, **30**, 6–9.
- 138 O. Arteaga, J. H. Freudenthal and B. Kahr, *J. Appl. Cryst.* 2012, **45**, 279–291.
- 139 S. M. Nichols, O. Arteaga, A. Martin and B. Kahr, *J. Opt. Soc. Am.* 2015, **32**, 2049–2057.
- 140 S. M. Nichols, Dissertation, New York University, 2018.
- 141 S. M. Nichols, O. Arteaga, A. T. Martin and B. Kahr, *Appl. Surf. Sci.* **2017**, **421PB**, 571–577.
- 142 S. M. Nichols, O. Arteaga, A. Martin and B. Kahr, *J. Opt. Soc. Am.* **2015**, **32**, 2049–2057.
- 143 S. R. Cloude, *Optik (Stuttgart)*, 1986, **7**, 26–36.
- 144 K. Postava, T. Yamaguchi, and R. Kantor, *Appl. Opt.* 2002, **41**, 2521–2531.
- 145 O. Arteaga, *Opt. Lett.* 2015, **40**, 4277–4280.
- 146 A. G. Shtukenberg, A. Gujral, E. Rosseeva, X. Cui and B. Kahr, *CrystEngComm*, 2015, **17**, 8817–8824.
- 147 A. N. Winchell, *The optical properties of organic compounds*, Academic Press, New York, 1954.
- 148 J. Freudenthal, Dissertation, New York University, 2011.
- 149 K. Nakagawa, A. T. Martin, S. M. Nichols, V. L. Murphy, B. Kahr and T. Asahi, *J. Phys. Chem. C* **2017**, **121**, 25494–25502.
- 150 von Lang, *V. S. B. Akad. Wiss. Wien, II*, 1872, **65**, 30.
- 151 W. C. G. Baldwin, *Proc. R. Soc. Lon. A*, 1938, **167**, 539–554.
- 152 S. Nichols, A. Martin, J. Choi and B. Kahr, *Chirality*, 2016, **28**, 460–465.
- 153 A. T. Martin, M. Tan, S. M. Nichols, E. L. Timothy and B. Kahr, *Chirality*, 2018, **30**, 841–849.
- 154 A. Matsumoto, T. Ide, Y. Kaimori, S. Fujiwara and K. Soai, *Chem. Lett.* 2015, **44**, 688–690.
- 155 A. T. Martin, S. M. Nichols, M. Tan, S. Li and B. Kahr, *J. Appl. Cryst.* 2017, **50**, 1117–1124.
- 156 A. Shtukenberg and Y. O. Punin, *Optically Anomalous Crystals*, (B. Kahr, ed.) Springer Series in Solid State Science, Springer, Dordrecht, 2007.
- 157 B. Kahr and J. M. McBride, *Angew. Chem. Int. Ed. Engl.* **1992**, **31**, 1–26.
- 158 S. A. Kim, C. Griewatsch and H. Küppers, *Zeit. Kristallogr.* 1993, **208**, 219–222.
- 159 A. Cyphersmith, S. Surampudi, M. J. Casey, K. Jankowski, D. Venkataraman and M. D. Barnes, *J. Phys. Chem. A*, 2012, **116**, 5349–5352.
- 160 M. D. Barnes, R. H. Paradise, E. Swain, D. Venkataraman and N. I. Hammer, *J. Phys. Chem. A*, 2009, **113**, 9757–9758.
- 161 A. Cohen and Y. Tang, *J. Phys. Chem. A*, 2009, **113**, 9759–9759.
- 162 S. Furumaki, Y. Yabiku, S. Habuchi, Y. Tsukatani, D. A. Bryant and M. Vacha, *J. Phys. Chem. Lett.* 2012, **3**, 3545–3549.
- 163 C. Isborn, K. Claborn and B. Kahr, *J. Phys. Chem. A* 2007, **111**, 7800–7804.
- 164 P. L. Polavarapu and D. K. Chakraborty, *Chem. Phys.* 1999, **240**, 1–8.

- 165 A. B. Grishanin and V. N. Zadkov, *J. Exp. Theor. Phys.* 1999, **89**, 669-676.
- 166 K. Ruud and T. Helgaker, *Chem. Phys. Lett.* 2002, **352**, 533-539.
- 167 P. Norman, K. Ruud and T. J. Helgaker, *Chem. Phys.* 2004, **120**, 5027-5035.
- 168 E. A. Zhelgovskaya and G. G. Malenkov, *Russ. Chem. Rev.* 2006, **75**, 57-76.
- 169 V. L. Murphy and B. Kahr, *J. Am. Chem. Soc.* 2015, **137**, 5177-5183.
- 170 V. L. Murphy, Dissertation, New York University, 2015.
- 171 V. L. Murphy, A. Reyes and B. Kahr, *J. Am. Chem. Soc.* 2016, **138**, 25-27.
- 172 W. Kauzmann, *Quantum Chemistry*, Academic Press, New York, 1954.
- 173 V. L. Murphy, C. Farfan and B. Kahr, *Chirality*, 2018, **30**, 325-331.
- 174 H. Zhong, Z. H. Levine, D. C. Allan and J. W. Wilkins, *Phys. Rev. Lett.* 1992, **69**, 379-382.
- 175 H. Zhong, Z. H. Levine, D. C. Allan and J. W. Wilkins, *Phys. Rev. B: Condens. Matter Mater. Phys.* 1993, **48**, 1384-1403.
- 176 T. Balduf and M. Caricato, *J. Phys. Chem. C* 2019, **123**, 4329-4340.
- 177 Lahiri, P., K. B. Wiberg, P. H. Vaccaro, M. Caricato and T. D. Crawford, *Angew. Chem.* **2014**, *126*, 1410-1413.
- 178 M. Rérat, B. Kirtman, *J. Chem. Theory Comput.* **2021**, *17*, 4063-4076.
- 179 T. E. Wood and A. Thompson, *Chem. Rev.* 1997, **107**, 1831-1861.
- 180 N. Boens, V. Leen and W. Dehaen, *Chem. Soc. Rev.* 2012, **41**, 1130-1172.
- 181 V. N. Vapnik, *IEEE Trans. Neural Net.* 1999, **10**, 988-999.
- 182 O. Arteaga, Z. El-Hachemi, A. Canillas and J. Ribó, *Thin Solid Films*, 2011, **519**, 2617-2623.
- 183 S. M. Nichols, J. H. Freudenthal, O. Arteaga and B. Kahr, *SPIE Sensing Technology+ Applications*, **2014**, 909912-909912-10.
- 184 O. Arteaga, M. Baldrís, J. Antó, A. Canillas, E. Pascual and E. Bertran, *Appl. Opt.* 2014, **53**, 2236-2245.
- 185 M. H. Smith, *Appl. Opt.*, 2002, **41**, 2488-2493.
- 186 M. A. Geday and A. M. Glazer, *J. Appl. Cryst.* 2002, **35**, 185-190.
- 187 Y. Shindo and Y. Oda, *Appl. Spectr.* 1992, **46**, 1251-1259.
- 188 O. Arteaga and S. Nichols, *J. Opt. Soc. Am. A*, 2018, **35**, 1254-1260.
- 189 J. Soni, H. Purwar, H. Lakhotia, S. Chandel, C. Banerjee, U. Kumar and N. Ghosh, *Opt. Exp.* 2013, **21**, 15475.
- 190 N. Mazumder, J. Qiu, F.-J. Kao and A. Diaspro, *J. Opt.* 2017, **19**, 025301.
- 191 K. Maji, S. Saha, R. Dey, N. Ghosh and D. Haldar, *J. Phys. Chem. C*, 2017, **121**, 19519-19529.
- 192 O. Arteaga, S. Nichols, V. Murphy, Y. Portorreal, C. Hu and B. Kahr, *Am. Cryst. Assoc. Transactions*, 2012, **43**, <http://www.amercrystalassn.org/2012-transactions>.
- 193 Y. Bing, D. Selassie, R. H. Paradise, C. Isborn, N. Kramer, M. Sadilek, W. Kaminsky and B. Kahr, *J. Am. Chem. Soc.* 2010, **132**, 7454-7465.
- 194 Y. Bing, W. Kaminsky, B. Kahr and D. Viterbo, *Angew. Chem. Int. Ed. Engl.* 2009, **48**, 2-8.
- 195 K. Claborn, A.-S. Chu, S.-H. Jang, F. Su, W. Kaminsky and B. Kahr, *Cryst. Growth Des.* 2005, **5**, 2117-2123.
- 196 W. Kaminsky, J. Herreros-Cédres, M. Geday and B. Kahr, *Chirality*, 2004, **16**, S55-S61.
- 197 W. Kaminsky, M. Geday, J. H. Cedres and B. Kahr, *J. Phys. Chem. A*, 2003, **107**, 2800-2807.
- 198 B. Kahr and R. W. Gurney, *Chem. Rev.* 2001, **101**, 893-951.
- 199 B. Kahr, A. Shtukenberg, *CrystEngComm*, 2016, **18**, 8988-8998.
- 200 S. M. Nichols, M. Tan, A. Martin, E. Timothy and B. Kahr arXiv:1710.09943 [physics.optics]
- 201 S. F. Boys, *Proc. Roy. Soc., Ser. A*, 1934, **144**, 65-675.
- 202 M. Tan, W. Jiang, A. T. Martin, A. G. Shtukenberg, M. D. McKee, B. Kahr, *Chem. Commun.* 2020, **56**, 7353-7356
- 203 L. Helmbrecht, M. Tan, R. Röhrich, B. Ortiz Kessels, F. Koenderink, B. Kahr and W. L. Noorduin, *Adv. Funct. Mater.* 2019, 1908218: 1-5.
- 204 H.-M. Ye, M. Tan, J. Freudenthal and B. Kahr, *Macromol.* 2019, **2**, 8514-8520.
- 205 X. Cui, S. Nichols, O. Arteaga, J. Freudenthal, F. Paula, A. G. Shtukenberg and B. Kahr, *J. Am. Chem. Soc.* 2016, **138**, 12211-12218.
- 206 X. Cui, A. Shtukenberg, J. Freudenthal, S. M. Nichols and B. Kahr *J. Am. Chem. Soc.* 2014, **136**, 5481-5490. 2
- 207 E. Gunn, R. Sours, J. B. Benedict, W. Kaminsky and B. Kahr, *J. Am. Chem. Soc.* 2006, **128**, 14234-14235.
- 208 A. Fang and M. Haataja, *Phys. Rev. E* 2105, **92**, 042404.
- 209 M. Schäferling, *Chiral Nanophotonics*, Springer, Stuttgart, 2017.
- 210 O. Arteaga, J.-S. Parramon, S. Nichols, B. Maoz, A. Canillas, S. Bosch, G. Markovich and B. Kahr, *Opt. Exp.* 2016, **24**, 2242-2252.
- 211 S. M. Nichols, O. Arteaga, B. M. Maoz, G. Markovich and B. Kahr *SPIE NanoScience + Engineering*, 2014, 91631W-91631W-10.
- 212 O. Arteaga, B. M. Maoz, S. Nichols, G. Markovich and B. Kahr, *Opt. Exp.* 2014, **22**, 13719-13732.
- 213 L. Nafie, *Vibrational Optical Activity: Principles and Applications*, Wiley, New York, 2011.
- 214 D. Sidler, P. Bleiziffer and S. Riniker, *J. Chem. Theory Comput.* 2019, **15**, 2492-2503.
- 215 X. Mu, X. Chen, J. Wang and M. Sun, *J. Phys. Chem. A* 2019, **123**, 8071-8081.
- 216 J. C. Wilson, P. Gutsche, S. Hermann, S. Burger and K. M. McPeak, *Opt. Exp.* 2019, **27**, 5097.
- 217 Y. Tang and A. E. Cohen, *Phys. Rev. Lett.* 2010, **104**, 163901.
- 218 Y. Tang and A. E. Cohen, *Science*, **332**, 333-336, 2011.

219 E. Hendry, T. Carpy, J. Johnston, M. Popland, R. V. Mikhaylovskiy, A. J. Laphorn, S. M. Kelly, L. D. Barron, N. Gadegaard and M. Kadodwala, *Nature Nanotech.* 2010, **5**, 783-787.